

Synthesis of Niobia Nanocrystals with Controlled Morphology

Edson R. Leite,* Cristiane Vila, Jefferson Bettini,[†] and Elson Longo

Department of Chemistry, Federal University of São Carlos, 13565-905 São Carlos, SP, Brazil, and National Laboratory of Synchrotron Light (LNLS), Campinas, SP, Brazil

Received: July 6, 2006

In this work, TT niobia-phase nanocrystals with controlled morphology were obtained by the hydrothermal treatment of a niobium peroxo complex precursor at very low temperatures. The materials obtained by this route presented a very high surface area (ranging from 79 to 327 m²/g), disordered NbO₆, NbO₇, and NbO₈ polyhedra, Nb–O superficial sites, and a superficial OH group, which must have ensured the acidic characteristics of this oxide.

Niobium pentoxide, or niobia (Nb₂O₅), possesses outstanding chemical and physical properties which make this oxide promising for application in catalysis¹ and photoelectrochemical² and electrochromic devices.³ In the past few years, niobia-based systems have received special attention due to their catalytic activity in several important chemical processes, particularly when high acidity and a water-tolerant property is required.¹ It is well-known that the acidic property of niobia is responsible for high catalytic activity in several reactions and that this acidity is related to the presence of distorted NbO₆, NbO₇, and NbO₈ polyhedra.⁴ Consequently, high catalytic activity is normally observed in high-surface-area amorphous or disordered hydrous niobium pentoxide with the general formula of Nb₂O₅·*n*H₂O (also known as niobic acid). The preparation of well-ordered niobia nanocrystals with high surface area and acidic surface characteristics still represents a challenge. For catalytic purposes, niobia is usually prepared by the hydrolysis of niobium ethoxide or NbCl₅, followed by crystallization at around 500 °C. Only recently has a new chemical synthesis approach using a nonaqueous⁵ and polyol-mediated method⁶ been developed to process well-ordered niobia nanocrystals at a low temperature of crystallization (lower than 200 °C). The crystallization process can be considered the critical step in the synthesis of metal oxide nanocrystals, and to avoid the inherent problems associated with crystallization promoted by heat treatment, such as loss of superficial hydroxyl groups and surface area, the best strategy is to promote crystallization under hydrothermal conditions. However, the hydrothermal strategy requires the use of an adequate precursor. In this paper, we present a novel chemical route to process niobia nanocrystals based on the hydrothermal treatment of niobium peroxo complex (NPC) in an aqueous solution. This novel approach allows for good control of the nanocrystal morphology as well as a crystallization process that does not eliminate the hydroxyl group, resulting in a material with high surface area and acidic sites.

The niobia nanocrystals were synthesized by hydrothermal treatment of NPC in an aqueous solution. Following a typical

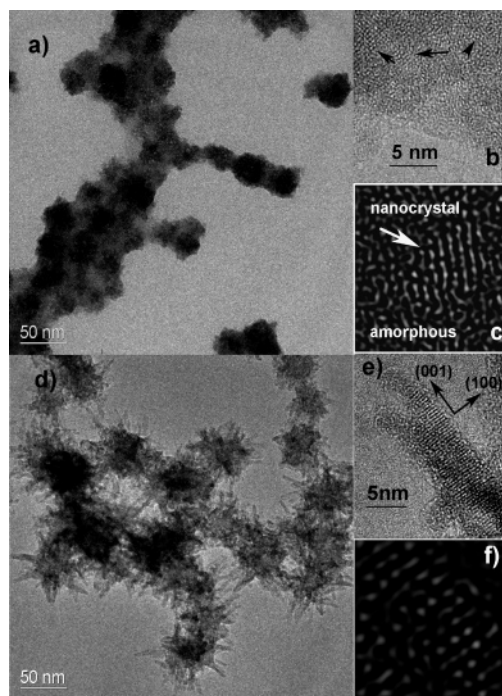


Figure 1. HRTEM images: images (a–c) correspond to niobia crystallized at 120 °C; images (d–f) correspond to niobia crystallized at 140 °C. Images (c) and (f) are reconstructed lattice images.

procedure, 8.00 g of ammonium niobium oxalate (general formula NH₄[NbO(C₂O₄)₂(H₂O)₂]·*n*H₂O supplied by CBMM, Brazil) were dissolved in 100 mL of high-purity water. In this step, a transparent colorless solution was obtained. Hydrogen peroxide (30% in vol.) was then added (10 mol/mol of Nb), resulting in a transparent yellow solution which indicated the formation of the NPC solution.⁷ This solution was poured into a bottle with an autoclavable screw cap. The bottle was then placed in a regular laboratory oven and subjected to a constant temperature (120 and 140 °C) for several hours. During the hydrothermal treatment, the yellow solution became colorless with the release of gas, indicating decomposition of the NPC, followed by the precipitation of a fine white particulate material.

* derl@power.ufscar.br.

[†] LNLS.

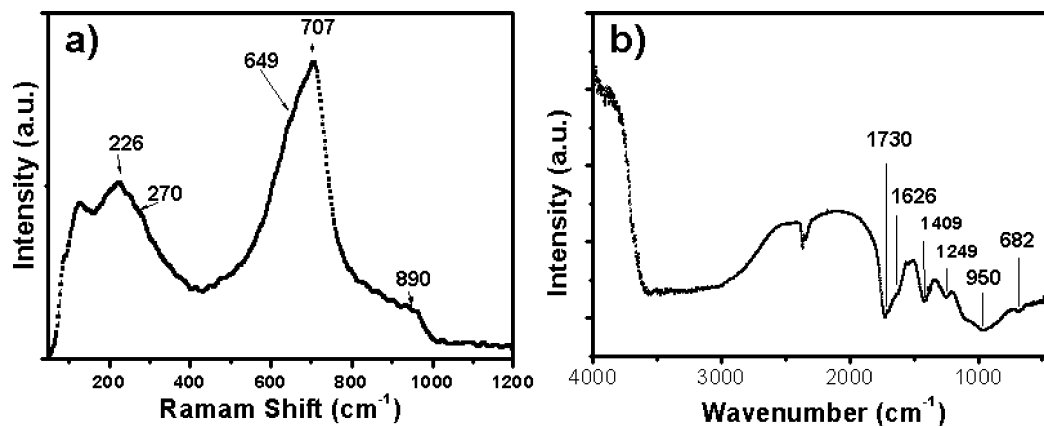


Figure 2. (a) FT-Raman of niobia crystallized at 140 °C. (b) DRIFT spectrum of niobia crystallized at 140 °C.

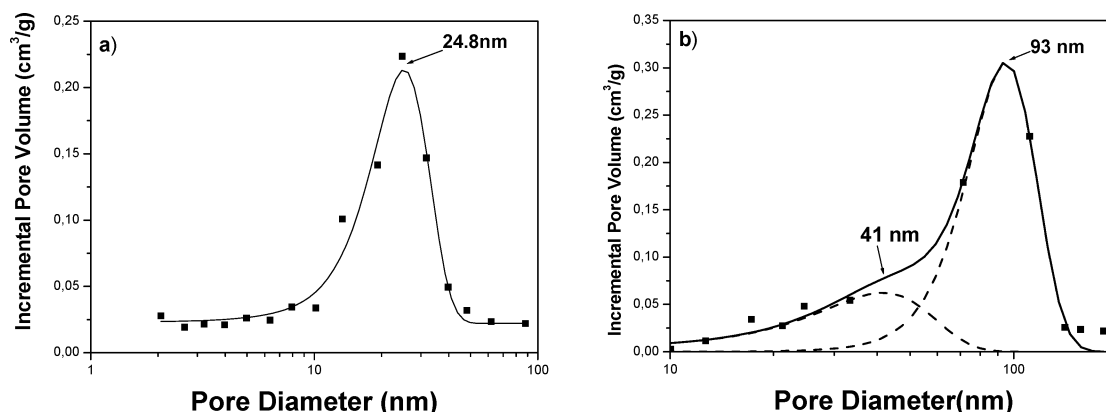


Figure 3. Pore size distribution curves, obtained by BJH method. A Gaussian function was used to fit the pore size distribution. (a) Niobia treated at 120 °C; (b) niobia treated at 140 °C.

The precipitated powder was centrifuged and washed in distilled water until the residual oxalate ions were completely eliminated (which was determined by a qualitative lead nitrate test). The resulting product was dried under low pressure ($\sim 10^{-2}$ Pa, at 60 °C, for 180 min) and characterized by high-resolution transmission electron microscopy (HRTEM, at 300 kV), X-ray diffraction (XRD; CuK α radiation), diffuse reflectance infrared Fourier transform (DRIFT) spectroscopy, and Raman spectroscopy (FT-Raman, excitation line of 1067 nm with 10 mV of power). Measurement of the surface area, hysteresis adsorption–desorption curve, and pore size distribution of the dry powder were obtained by nitrogen adsorption–desorption isothermal analysis.

The HRTEM characterization of the niobia treated at 120 and 140 °C presented interesting results about the crystallization and growth mechanism. The low-magnification HRTEM image (Figure 1a) of the niobia treated at 120 °C shows the presence of agglomerates composed of spherical particles. The high-magnification HRTEM image in Figure 1b shows that the spherical particles consist of small nanocrystals with sizes ranging from 1 to 3 nm (indicated by black arrows) and also reveals an amorphous region. Figure 1c illustrates a reconstructed lattice image, showing a detailed image of a nanocrystal embedded in the amorphous matrix. This result suggests a crystallization process based on a classical nucleation–growth mechanism. Increasing the treatment temperature to 140 °C led to a remarkable modification in the particle morphology, as indicated in the low-magnification HRTEM image of Figure 1d, which shows the presence of an agglomeration of nanorods. The high-magnification HRTEM image of Figure 1e reveals the presence of well-crystallized nanorods of TT-niobia phase, with preferential growth in the [001] direction. An XRD analysis

of this material confirmed the presence of TT-niobia phase with preferential orientation in the [001] direction. Figure 1f shows a reconstructed lattice image of the nanorods, revealing different degrees of misorientation and point defects, which may have been generated by imperfect attachment between nanocrystals, suggesting that the nanorod growth process is related to the oriented attachment mechanism (OA).⁸ The OA mechanism can occur by collision, collision and rotation,⁹ and solid-state rotation between nanocrystals.¹⁰ In the present study, the OA mechanism must have been controlled by solid-state rotation, since an amorphous-to-crystalline phase transformation was observed, originating a solid–solid interface among the nanocrystals. The rotation may have occurred to decrease the angle of misorientation, changing the orientation of the particles. When the particles assumed a coherent particle–particle boundary, the particle boundary must have migrated, resulting in a single, larger crystalline particle.

Figure 2 shows the FT-Raman and DRIFT spectra of the niobia crystallized at 140 °C. The FT-Raman spectrum (Figure 2a) shows a broad and asymmetric band in the region of 600–800 cm^{-1} assigned to the symmetric stretching mode of the Nb–O polyhedra (presence of disordered NbO₆, NbO₇, and NbO₈ polyhedra). Note, also, the Raman band in the range 830–1000 cm^{-1} assigned to the symmetric stretching mode of Nb–O superficial sites and bands at low Raman shift, which are characteristic of the bending modes of Nb–O–Nb linkages.¹¹ This Raman spectrum confirms the presence of the TT-niobia phase and is similar to the spectrum obtained for hydrous niobium pentoxide calcined in the temperature range 400–600 °C.¹¹ The TT-niobia phase is metastable and can be stabilized by anion impurities.¹² The DRIFT spectrum of the material crystallized at 140 °C shows the presence of superficial carboxyl

(vibrations at 1730, 1630, 1409 cm^{-1}), OH (3590–2960 cm^{-1}), and O–O (950 and 682 cm^{-1}) groups, which can contribute to stabilizing the TT-niobia phase.

The niobia treated at 120 °C showed a Brunauer–Emmett–Teller (BET) surface area of 327 m^2/g , and the niobia treated at 140 °C showed a BET surface area of 78.9 m^2/g . Both materials presented a typical adsorption–desorption isothermal hysteresis characteristic of mesoporous solids. Pore-size distribution curves, obtained by the Barret-Joyner-Halenda (BJH) method, by considering desorption curves, are shown in Figure 3. The material treated at 120 °C showed a monomodal pore size distribution with a most frequent pore diameter of 24.8 nm. On the other hand, the material treated at 140 °C showed a bimodal pore size distribution, with most frequent pore diameters of 41 nm and 93 nm. These differences in surface area and pore size distribution must be due to the different morphologies induced by the growth process. The high surface area and the mesoporous nature reported here for niobia are desirable properties for solid catalysts and electrochemistry devices.

In summary, TT-niobia phase nanocrystals with controlled morphology were obtained by the hydrothermal treatment of an NPC precursor at very low temperatures. The materials obtained by this route presented a very high surface area, disordered NbO_6 , NbO_7 , and NbO_8 polyhedra, Nb–O superficial

sites, and a superficial OH group, which must have ensured the acidic characteristics of this oxide. The materials reported in this communication present interesting catalytic, electrochemical, and electrochromic properties that will undoubtedly be further explored. A similar synthesis approach will be used to prepare TiO_2 and ZrO_2 nanocrystals.

Acknowledgment. The financial support of FAPESP and CNPq (both Brazilian agencies) is gratefully acknowledged. The HRTEM facilities were provided by the LNLS (National Laboratory of Synchrotron Light), Campinas, SP, Brazil.

References and Notes

- (1) Taanabe, K. *Catal. Today* **2003**, 78, 65.
- (2) Graetzel, M. *Nature (London)* **2001**, 414, 338.
- (3) Aegerter, M. A. *Sol. Energy Mater. Sol. Cell* **2001**, 68, 401.
- (4) Jehng, J.-M.; Wachs, I. E. *Catal. Today* **1990**, 8, 37.
- (5) Pina, N.; Antonietti, M.; Niederberger, M. *Colloids Surf., A* **2004**, 250, 211.
- (6) Feldmann, C.; Jungk, H.-O. *Angew. Chem., Int. Ed.* **2001**, 40, 359.
- (7) Narendar, Y.; Messing, G. L. *Chem. Mater.* **1997**, 9, 580.
- (8) Penn, R. L.; Banfield, J. F. *Science* **1998**, 281, 969.
- (9) Ribeiro, C.; Lee, E. J. H.; Longo, E.; Leite, E. R. *ChemPhysChem* **2005**, 6, 690.
- (10) Ribeiro, C.; Lee, E. J. H.; Giraldo, T. R.; Aguiar, R.; Longo, E.; Leite, E. R. *J. Appl. Phys.* **2005**, 97, 024313.
- (11) Jehng, J.-M.; Wachs, I. E. *Chem. Mater.* **1991**, 3, 100.
- (12) Weimann, J.; Ko, E. I. *Chem. Mater.* **1989**, 1, 187.